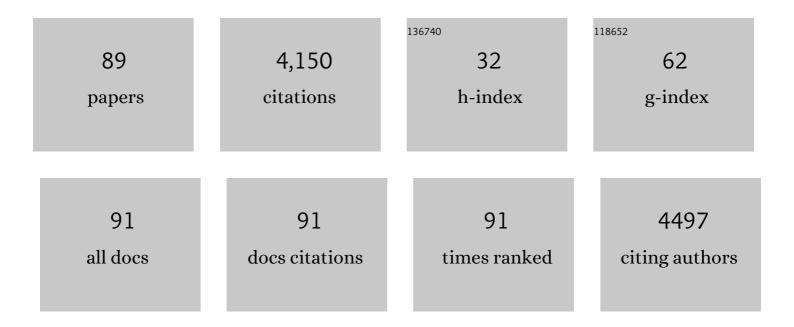
Konstantin Pervushin

List of Publications by Year in descending order

Source: https://exaly.com/author-pdf/5455445/publications.pdf Version: 2024-02-01



#	Article	IF	CITATIONS
1	TROSY-type Triple-Resonance Experiments for Sequential NMR Assignments of Large Proteins. Journal of the American Chemical Society, 1999, 121, 844-848.	6.6	315
2	Transverse Relaxation-Optimized Spectroscopy (TROSY) for NMR Studies of Aromatic Spin Systems in13C-Labeled Proteins. Journal of the American Chemical Society, 1998, 120, 6394-6400.	6.6	288
3	Structure and Inhibition of the SARS Coronavirus Envelope Protein Ion Channel. PLoS Pathogens, 2009, 5, e1000511.	2.1	216
4	Longitudinal1H Relaxation Optimization in TROSY NMR Spectroscopy. Journal of the American Chemical Society, 2002, 124, 12898-12902.	6.6	166
5	TROSY and CRINEPT: NMR with large molecular and supramolecular structures in solution. Trends in Biochemical Sciences, 2000, 25, 462-468.	3.7	159
6	Impact of Transverse Relaxation Optimized Spectroscopy (TROSY) on NMR as a technique in structural biology. Quarterly Reviews of Biophysics, 2000, 33, 161-197.	2.4	150
7	An enzymatic molten globule: Efficient coupling of folding and catalysis. Proceedings of the National Academy of Sciences of the United States of America, 2004, 101, 12860-12864.	3.3	128
8	Solution NMR studies of the integral membrane proteins OmpX and OmpA fromEscherichia coli. FEBS Letters, 2001, 504, 173-178.	1.3	123
9	NMR Assignment and Secondary Structure Determination of an Octameric 110 kDa Protein Using TROSY in Triple Resonance Experiments. Journal of the American Chemical Society, 2000, 122, 7543-7548.	6.6	121
10	Amino Acid Modified Xanthone Derivatives: Novel, Highly Promising Membrane-Active Antimicrobials for Multidrug-Resistant Gram-Positive Bacterial Infections. Journal of Medicinal Chemistry, 2015, 58, 739-752.	2.9	109
11	The Small Hydrophobic Protein of the Human Respiratory Syncytial Virus Forms Pentameric Ion Channels. Journal of Biological Chemistry, 2012, 287, 24671-24689.	1.6	106
12	Hydrogen bond guidance and aromatic stacking drive liquid-liquid phase separation of intrinsically disordered histidine-rich peptides. Nature Communications, 2019, 10, 5465.	5.8	105
13	The Molecular Basis of Distinct Aggregation Pathways of Islet Amyloid Polypeptide. Journal of Biological Chemistry, 2011, 286, 6291-6300.	1.6	104
14	Structure and dynamics of a molten globular enzyme. Nature Structural and Molecular Biology, 2007, 14, 1202-1206.	3.6	102
15	Improved sensitivity and coherence selection for [15N,1H]-TROSY elements in triple resonance experiments. Journal of Biomolecular NMR, 1999, 15, 181-184.	1.6	94
16	A novel strategy for the assignment of side-chain resonances in completely deuterated large proteins using 13C spectroscopy. Journal of Biomolecular NMR, 2003, 26, 167-179.	1.6	88
17	Structural Flexibility of the Pentameric SARS Coronavirus Envelope Protein Ion Channel. Biophysical Journal, 2008, 95, L39-L41.	0.2	71
18	TROSY NMR with partially deuterated proteins. Journal of Biomolecular NMR, 2001, 20, 177-180.	1.6	67

#	Article	IF	CITATIONS
19	Structure-Dependent Charge Density as a Determinant of Antimicrobial Activity of Peptide Analogues of Defensin. Biochemistry, 2009, 48, 7229-7239.	1.2	64
20	[13C,13C]- and [13C,1H]-TROSY in a Triple Resonance Experiment for Riboseâ [~] 'Base and Intrabase Correlations in Nucleic Acids1. Journal of the American Chemical Society, 2001, 123, 658-664.	6.6	61
21	NMR Structure of the Heme Chaperone CcmE Reveals a Novel Functional Motif. Structure, 2002, 10, 1551-1557.	1.6	61
22	[13C]-constant-time [15N,1H]-TROSY-HNCA for sequential assignments of large proteins. Journal of Biomolecular NMR, 1999, 14, 85-88.	1.6	56
23	Molecular simulations suggest how a branched antimicrobial peptide perturbs a bacterial membrane and enhances permeability. Biochimica Et Biophysica Acta - Biomembranes, 2013, 1828, 1112-1121.	1.4	56
24	Unusual Hemeâ^'Histidine Bond in the Active Site of a Chaperone. Journal of the American Chemical Society, 2005, 127, 3716-3717.	6.6	55
25	Identification of a Polyoxometalate Inhibitor of the DNA Binding Activity of Sox2. ACS Chemical Biology, 2011, 6, 573-581.	1.6	48
26	A new strategy for backbone resonance assignment in large proteins using a MQ-HACACO experiment. Journal of Biomolecular NMR, 2003, 25, 147-152.	1.6	47
27	Structural Role of a Buried Salt Bridge in the 434 Repressor DNA-binding Domain. Journal of Molecular Biology, 1996, 264, 1002-1012.	2.0	45
28	Alternate rRNA secondary structures as regulators of translation. Nature Structural and Molecular Biology, 2011, 18, 169-176.	3.6	44
29	Determination of h2J(NN) and h1J(HN) coupling constants across Watson-Crick base pairs in the Antennapedia homeodomain-DNA complex using TROSY. Journal of Biomolecular NMR, 2000, 16, 39-46.	1.6	43
30	Residual Structure in Islet Amyloid Polypeptide Mediates Its Interactions with Soluble Insulin. Biochemistry, 2009, 48, 2368-2376.	1.2	42
31	DNA-mediated cooperativity facilitates the co-selection of cryptic enhancer sequences by SOX2 and PAX6 transcription factors. Nucleic Acids Research, 2015, 43, 1513-1528.	6.5	37
32	A novel fragment based strategy for membrane active antimicrobials against MRSA. Biochimica Et Biophysica Acta - Biomembranes, 2015, 1848, 1023-1031.	1.4	36
33	A Short Peptide Hydrogel with High Stiffness Induced by 3 ₁₀ â€Helices to βâ€Sheet Transition in Water. Advanced Science, 2019, 6, 1901173.	5.6	36
34	[15N,1H]/[13C,1H]-TROSY for simultaneous detection of backbone 15N-1H, aromatic 13C-1H and side-chain 15N-1H2 correlations in large proteins. Journal of Biomolecular NMR, 2000, 17, 195-202.	1.6	35
35	The use of TROSY for detection and suppression of conformational exchange NMR line broadening in biological macromolecules. , 2001, 20, 275-285.		34
36	Detection of C′,Cα correlations in proteins using a new time- and sensitivity-optimal experiment. Journal of Biomolecular NMR, 2005, 31, 273-278.	1.6	33

Konstantin Pervushin

#	Article	IF	CITATIONS
37	Structural Plasticity of Peptidylâ^'Prolyl Isomerase sFkpA Is a Key to Its Chaperone Function As Revealed by Solution NMRâ€. Biochemistry, 2006, 45, 11983-11991.	1.2	33
38	Progressive Structuring of a Branched Antimicrobial Peptide on the Path to the Inner Membrane Target. Journal of Biological Chemistry, 2012, 287, 26606-26617.	1.6	32
39	A Minimal Transmembrane β-Barrel Platform Protein Studied by Nuclear Magnetic Resonanceâ€,‡. Biochemistry, 2007, 46, 1128-1140.	1.2	31
40	Expression and purification of coronavirus envelope proteins using a modified β-barrel construct. Protein Expression and Purification, 2012, 85, 133-141.	0.6	31
41	Abundant neuroprotective chaperone Lipocalin-type prostaglandin D synthase (L-PGDS) disassembles the Amyloid-β fibrils. Scientific Reports, 2019, 9, 12579.	1.6	31
42	Structure and Dynamics in the Nucleosome Revealed by Solid‧tate NMR. Angewandte Chemie - International Edition, 2018, 57, 9734-9738.	7.2	30
43	Investigation of Ligand Binding and Protein Dynamics inBacillus subtilisChorismate Mutase by Transverse Relaxation Optimized Spectroscopyâ°'Nuclear Magnetic Resonanceâ€,â€j. Biochemistry, 2005, 44, 6788-6799.	1.2	29
44	Allotides: Proline-Rich Cystine Knot α-Amylase Inhibitors from <i>Allamanda cathartica</i> . Journal of Natural Products, 2015, 78, 695-704.	1.5	29
45	Modular peptides from the thermoplastic squid sucker ring teeth form amyloid-like cross-β supramolecular networks. Acta Biomaterialia, 2016, 46, 41-54.	4.1	29
46	Probing the rotor subunit interface of the ATP synthase from <i>llyobacter tartaricus</i> . FEBS Journal, 2008, 275, 4850-4862.	2.2	28
47	Solution Structure of the PAS Domain of a Thermophilic YybT Protein Homolog Reveals a Potential Ligand-binding Site. Journal of Biological Chemistry, 2013, 288, 11949-11959.	1.6	27
48	Deuterium Relaxation in a Uniformly15N-Labeled Homeodomain and Its DNA Complex1. Journal of the American Chemical Society, 1997, 119, 3842-3843.	6.6	26
49	Molecular dynamics simulations of a new branched antimicrobial peptide: A comparison of force fields. Journal of Chemical Physics, 2012, 137, 215101.	1.2	26
50	Simultaneous 1H- or 2H-, 15N- and multiple-band-selective 13C-decoupling during acquisition in 13C-detected experiments with proteins and oligonucleotides. Journal of Biomolecular NMR, 2005, 31, 1-9.	1.6	24
51	Structural and dynamic insights into substrate binding and catalysis of human lipocalin prostaglandin D synthase. Journal of Lipid Research, 2013, 54, 1630-1643.	2.0	24
52	Measurements of Side-Chain13Câ^'13C Residual Dipolar Couplings in Uniformly Deuterated Proteins. Journal of the American Chemical Society, 2004, 126, 2414-2420.	6.6	23
53	The Leucine Zipper Domains of the Transcription Factors GCN4 and c-Jun Have Ribonuclease Activity. PLoS ONE, 2010, 5, e10765.	1.1	23
54	Three-dimensional structure of <i>Megabalanus rosa</i> Cement Protein 20 revealed by multi-dimensional NMR and molecular dynamics simulations. Philosophical Transactions of the Royal Society B: Biological Sciences, 2019, 374, 20190198.	1.8	22

#	Article	IF	CITATIONS
55	NMR Spin State Exchange Spectroscopy Reveals Equilibrium of Two Distinct Conformations of Leucine Zipper GCN4 in Solution. Journal of the American Chemical Society, 2007, 129, 6461-6469.	6.6	21
56	Backbone resonance assignment in large protonated proteins using a combination of new 3D TROSY-HN(CA)HA, 4D TROSY-HACANH and 13C-detected HACACO experiments. Journal of Biomolecular NMR, 2003, 26, 69-77.	1.6	20
57	Antimicrobial activity profiles of Amphiphilic Xanthone derivatives are a function of their molecular Oligomerization. Biochimica Et Biophysica Acta - Biomembranes, 2018, 1860, 2281-2298.	1.4	18
58	The Cytoplasmic Domain of the Chloride Channel ClC-0: Structural and Dynamic Characterization of Flexible Regions. Journal of Molecular Biology, 2007, 369, 1163-1169.	2.0	17
59	Direct NMR observation and DFT calculations of a hydrogen bond at the active site of a 44 kDa enzyme. Journal of Biomolecular NMR, 2002, 24, 31-39.	1.6	16
60	Selectivity of stop codon recognition in translation termination is modulated by multiple conformations of GTS loop in eRF1. Nucleic Acids Research, 2012, 40, 5751-5765.	6.5	15
61	SideLink: Automated side-chain assignment of biopolymers from NMR data by relative-hypothesis-prioritization-based simulated logic. Journal of Magnetic Resonance, 2006, 181, 45-67.	1.2	14
62	Effect of position-specific single-point mutations and biophysical characterization of amyloidogenic peptide fragments identified from lattice corneal dystrophy patients. Biochemical Journal, 2017, 474, 1705-1725.	1.7	14
63	Molecular mechanisms of amyloid disaggregation. Journal of Advanced Research, 2022, 36, 113-132.	4.4	14
64	TROSY experiment for refinement of backbone psi and phi by simultaneous measurements of cross-correlated relaxation rates and 3,4J(H alpha HN) coupling constants. Journal of Biomolecular NMR, 2002, 24, 291-300.	1.6	13
65	Polychromatic Selective Population Inversion for TROSY Experiments with Large Proteins. Journal of the American Chemical Society, 2005, 127, 405-411.	6.6	13
66	pH-Dependent Interactions of Human Islet Amyloid Polypeptide Segments with Insulin Studied by Replica Exchange Molecular Dynamics Simulations. Journal of Physical Chemistry B, 2010, 114, 10176-10183.	1.2	12
67	Efficiency of High Magnetic Fields in Solid-state NMR. Chemistry Letters, 2016, 45, 209-210.	0.7	11
68	Observation of Individual Transitions in Magnetically Equivalent Spin Systems. Journal of the American Chemical Society, 2003, 125, 9566-9567.	6.6	10
69	Improved TROSY-HNCA experiment with suppression of conformational exchange induced relaxation. Journal of Biomolecular NMR, 2001, 21, 161-166.	1.6	9
70	Side-chain H and C resonance assignment in protonated/partially deuterated proteins using an improved 3D13C-detected HCC–TOCSY. Journal of Magnetic Resonance, 2005, 174, 200-208.	1.2	9
71	Benchmarking NMR experiments: A relational database of protein pulse sequences. Journal of Magnetic Resonance, 2010, 203, 129-137.	1.2	9
72	Trans-Hydrogen-Bond Scalar Couplings as a Source of Structural Constraints in NMR of Proteins: DFT Analysis. Helvetica Chimica Acta, 2002, 85, 3984-3993.	1.0	8

#	Article	IF	CITATIONS
73	Amyloid β chaperone — lipocalin-type prostaglandin D synthase acts as a peroxidase in the presence of heme. Biochemical Journal, 2020, 477, 1227-1240.	1.7	8
74	Utf1 contributes to intergenerational epigenetic inheritance of pluripotency. Scientific Reports, 2017, 7, 14612.	1.6	7
75	Matrixâ€Assisted Laser Desorption Ionization Mass Spectrometry Imaging of Key Proteins in Corneal Samples from Lattice Dystrophy Patients with TGFBI â€H626R and TGFBI â€R124C Mutations. Proteomics - Clinical Applications, 2019, 13, 1800053.	0.8	7
76	Domain Features of the Peripheral Stalk Subunit H of the Methanogenic A1AO ATP Synthase and the NMR Solution Structure of H1-47. Biophysical Journal, 2009, 97, 286-294.	0.2	6
77	Structural basis of RNA binding by leucine zipper GCN4. Protein Science, 2012, 21, 667-676.	3.1	6
78	NMR Structures of Salt-Refolded Forms of the 434-Repressor DNA-Binding Domain in 6 M Ureaâ€. Biochemistry, 2004, 43, 13937-13943.	1.2	5
79	Automatic assignment of protein backbone resonances by direct spectrum inspection in targeted acquisition of NMR data. Journal of Biomolecular NMR, 2008, 42, 77-86.	1.6	5
80	Letter to the Editor: Backbone HN, N, Cα, C′ and Cβchemical shift assignments and secondary structure of FkpA, a 245-residue peptidyl-prolyl cis/trans isomerase with chaperone activity. Journal of Biomolecular NMR, 2004, 28, 405-406.	1.6	4
81	Anticholinergic Drugs Interact With Neuroprotective Chaperone L-PGDS and Modulate Cytotoxicity of Aβ Amyloids. Frontiers in Pharmacology, 2020, 11, 862.	1.6	4
82	Measuring 1H–1H and 1H–13C RDCs in methyl groups: example of pulse sequences with numerically optimized coherence transfer schemes. Journal of Magnetic Resonance, 2005, 172, 36-47.	1.2	3
83	Comprehensive Analysis and Identification of the Human STIM1 Domains for Structural and Functional Studies. PLoS ONE, 2013, 8, e53979.	1.1	3
84	Collaborative development for setup, execution, sharing and analytics of complex NMR experiments. Journal of Magnetic Resonance, 2014, 239, 121-129.	1.2	2
85	Binding of a small molecule water channel inhibitor to aquaporin Z examined by solid-state MAS NMR. Journal of Biomolecular NMR, 2018, 71, 91-100.	1.6	2
86	Sequence-specific 1H, 13C and 15N resonance assignments of the rat liver fructose-2,6-bisphosphatase domain. Journal of Biomolecular NMR, 2003, 27, 281-282.	1.6	1
87	Structural characterization of eRF1 mutants indicate a complex mechanism of stop codon recognition. Scientific Reports, 2016, 6, 18644.	1.6	1
88	Polychromatic frequency encoding in indirect dimensions in NMR spectroscopy. Molecular Physics, 2013, 111, 765-770.	0.8	0
89	Extended Structure of Rat Islet Amyloid Polypeptide in Solution. Advances in Experimental Medicine and Biology, 2015, 827, 85-92.	0.8	0